



HAL
open science

How well can linear stability analysis predict the behavior of an outward valve brass instrument model ?

Lionel Velut, Christophe Vergez, Joël Gilbert, Mithra Djahanbani

► To cite this version:

Lionel Velut, Christophe Vergez, Joël Gilbert, Mithra Djahanbani. How well can linear stability analysis predict the behavior of an outward valve brass instrument model ?. 2015. hal-01245846v1

HAL Id: hal-01245846

<https://hal.science/hal-01245846v1>

Preprint submitted on 17 Dec 2015 (v1), last revised 22 Feb 2017 (v4)

HAL is a multi-disciplinary open access archive for the deposit and dissemination of scientific research documents, whether they are published or not. The documents may come from teaching and research institutions in France or abroad, or from public or private research centers.

L'archive ouverte pluridisciplinaire **HAL**, est destinée au dépôt et à la diffusion de documents scientifiques de niveau recherche, publiés ou non, émanant des établissements d'enseignement et de recherche français ou étrangers, des laboratoires publics ou privés.

How well can linear stability analysis predict the behavior of an outward valve brass instrument model ?

Lionel Velut¹, Christophe Vergez¹, Joël Gilbert², and Mithra Djahanbani¹

¹LMA, CNRS, UPR 7051, Aix-Marseille Univ., Centrale Marseille, F-13453
Marseille cedex 13, France.

²Laboratoire d'Acoustique de l'Université du Maine, UMR CNRS-6613, Avenue
Olivier Messiaen, 72085 LE MANS cedex 9, France

December 17, 2015

Abstract

A physical model of brass instrument is considered in this paper : a one degree-of-freedom outward striking valve for the lips, non-linearly coupled to a modal representation of the air column. It is studied through linear stability analysis of the equilibrium solution. This approach provides the threshold value of the blowing pressure at which an instability occurs, and the value of the frequency of this instability. The validity of the results of this method is theoretically limited to the neighborhood of the equilibrium solution. This paper checks the efficiency of linear stability analysis to understand the behavior of the model computed through time-domain simulations. As expected, a good agreement is observed between linear stability analysis and numerical simulations of the complete nonlinear model around the oscillation threshold. For blowing pressures far above the oscillation threshold, the picture is more contrasted. In most cases tested, a periodic regime coherent with the linear stability analysis results is observed, but over-blowing, quasi-periodicity and period-doubling also occur. Interestingly, linear stability analysis predicts the production of the pedal note by a trombone, for which only nonlinear hypotheses had been previously proposed. LSA also predicts the production of a saxhorn note that had never been documented, but known by musicians.

I Introduction

Linear Stability Analysis (LSA) can be used to analyze the behaviour of dynamical systems around equilibrium points (i.e. non-oscillating solutions). LSA consists in writing a linearized version of the system around a given equilibrium point. Its stability is then assessed by studying the response of the linearized system to harmonic perturbations.

LSA has already been applied to physical models of musical instruments: woodwind instruments [Wilson and Beavers, 1974, Silva et al., 2008, Karkar et al., 2012], flute-like instruments [Terrien et al., 2014] and brass instruments [Cullen et al., 2000, Silva et al., 2007]. By definition, the validity of the results of LSA is theoretically limited to the neighborhood of the equilibrium solution. However, recent results on flutes have highlighted that important features of periodic regimes such as their frequencies are explained by LSA [Terrien et al., 2014]. This paper examines how far LSA can be used to understand some aspects of the behavior of a physical model of brass instruments.

Physical models of brass instruments have been proposed in multiple studies [Elliott and Bowsher, 1982, Fletcher, 1993, Adachi and Sato, 1996b, Cullen et al., 2000, Campbell, 2004, Silva et al., 2007, Myers et al., 2012]. Since we are interested in studying a simple model, a one degree-of-freedom system to model the lips is retained: the outward-striking valve. For the same reason, the nonlinear propagation in the bore of the instrument responsible of "brassy sounds" at high sound levels [Myers et al., 2012] is ignored. The coupling by the blown air flow between the lips and the air column inside the bore is modelled through a classical nonlinear algebraic equation [Hirschberg et al., 1995]. This model is detailed in section A. Even such a simple model has more parameters to tune than the simplest models of woodwind instruments. The latter can indeed be written with respect to two dimensionless parameters only [Hirschberg et al., 1995, Dalmont et al., 1995, Taillard et al., 2010, Bergeot et al., 2013]. However, for each valve position, brass players are able to play on multiple acoustic modes (or registers) of the air column by modifying significantly the mechanical characteristics of their lips. Therefore, the lip dynamics cannot be ignored, which increases the number of parameters to tune. A bibliographical review is given in section B to give grounds for the values chosen for each parameter of the model. In section C, details are given on how LSA is applied to the model. In order to exhibit behaviors of the nonlinear model to compare with LSA results, many options are available. For instance, the Harmonic Balance Method gives a Fourier series approximation of the steady state of periodic regimes, including unstable ones [Gilbert et al., 1989, Menguy and Gilbert, 2000, Cochelin and Vergez, 2009]. Since the pioneering work of [McIntyre et al., 1983, Schumacher, 1981], it is also possible to carry out time-domain simulations at moderate computational cost, providing access to transients and possibly non-periodic solutions. This latter approach is retained (see section D). Section III confronts the results of LSA and numerical simulation for different sets of parameter values. Different registers are explored, but also less common regimes such as quasi-periodicity and period-doubling. In section IV, we focus on the lowest register of brass instruments, called the pedal note, a particularly interesting case where LSA provides unexpected information on numerical simulation results.

II Tools

A Brass instrument model

In most wind instruments [Fletcher, 1993], including brass instruments [Cullen et al., 2000, Elliott and Bowsher, 1982, Yoshikawa, 1995], the oscillation relies on the coupling between a non-linear exciter and a linear resonator. More generally, the closed-loop system representation shown in fig. 1 is widely used by the musical acoustics community, since the seminal work of von Helmholtz [von Helmholtz, 1954, McIntyre et al., 1983].

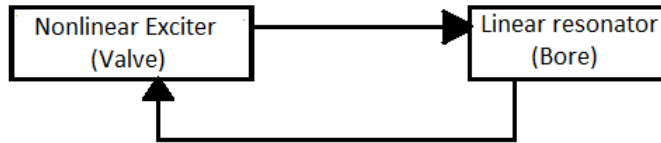


Figure 1: Closed-loop model suitable for the description of most self-sustained musical instruments. Self-sustained oscillations are generated by the coupling between a localized nonlinear exciter and a (linear) resonator. For brass instrument, the lip reed provides the excitation while the resonator is the air inside the bore. Both elements are non-linearly coupled through the air flow between the lips.

For brass instruments, the exciter consists of the lips of the musician, represented by a linear, oscillator-like valve, linking the height between the lips $h(t)$ and the pressure difference across the lips $\delta p(t) = p_b - p(t)$. p_b is the blowing pressure (pressure in the mouth, assumed to be static) and $p(t)$ the oscillating pressure signal inside the mouthpiece (the input of the bore). The resonator is the bore of a trombone or a saxhorn (see section IV.B). These resonators are represented by their input impedance, which links, in the frequency domain, the pressure at the input of the resonator $P(\omega)$ and the acoustic flow at the same point $U(\omega)$:

$$Z(\omega) = \frac{P(\omega)}{U(\omega)}. \quad (1)$$

Those two linear elements are non-linearly coupled by the airflow through the lip channel. The nonlinear exciter of fig. 1 consists in this coupling and the lip valve. The air jet is assumed to be laminar in the lip channel, but turbulent in the mouthpiece, all its kinetic energy being dissipated without pressure recovery. Applying the Bernoulli law and the mass conservation law between the mouth and the lip channel gives the following expression of the flow between lips, depending on the pressure difference and the height of the lip channel [Hirschberg et al., 1995]:

$$u(t) = \sqrt{\frac{2}{\rho}} L h(t) \sqrt{p_b - p(t)}, \quad (2)$$

with $u(t)$ being the airflow rate (m^3s^{-1}), $h(t)$ the height of the channel between the lips (m), $\rho = 1.19\text{kg}\cdot\text{m}^{-3}$ the density of the air at 20°C and L the width of the lip channel (m).

A one degree of freedom valve (referred to hereafter as "1-DOF valve") [Fletcher, 1993] is enough to model the lips for common playing situations [Yoshikawa, 1995] with a tractable number of

parameters. Two kinds of 1-DOF valves can be considered : "striking outward", which tends to open when δp grows, and "striking inward" which presents the opposite behavior.

While inward-striking valves are globally recognized as a satisfying way to represent woodwind reeds [Wilson and Beavers, 1974, Dalmont et al., 1995] there is no consensus about the modeling of the lip reed, as neither the outward nor the inward valve model reproduces all the behaviors observed with real musicians. Particularly, a trombonist (or any brass player) is able to get a playing frequency f_{osc} above and below the resonance frequency $f_{ac,n}$ of the n^{th} acoustic mode of the instrument [Campbell, 2004]. Whereas a 1-DOF inward or outward model is limited to playing frequencies respectively below or above $f_{ac,n}$ to meet the regeneration condition explained in [Elliott and Bowsher, 1982]. Moreover, measurements of the mechanical response of artificial [Cullen et al., 2000] and natural lips [Newton et al., 2008] revealed the coexistence of both inward and outward resonances: this allows f_{osc} to be below or above $f_{ac,n}$ at threshold. However, situations where f_{osc} is below $f_{ac,n}$ (inward-striking behavior) are mostly specific to some musical effects: for regular playing situations, the playing frequency is above f_{ac} . Moreover, real human lips open when air is blown, which is clearly an outward behavior. The relevance of this choice will be reinforced throughout this article, by comparing the results of the model analysis to known behaviors of brasswinds.

The outward-striking valve gives a relation between the height of the channel between the lips and the pressure difference across the lips :

$$\frac{d^2h}{dt^2} + \frac{\omega_l}{Q_l} \frac{dh}{dt} + \omega_l^2(h - h_0) = \frac{1}{\mu}(p_b - p(t)), \quad (3)$$

where $\omega_l = 2\pi f_l$ (rad/s) is the lips resonance angular frequency; Q_l the (dimensionless) quality factor of the lips; h_0 the value of $h(t)$ at rest; μ an equivalent surface mass of the lips (kg.m^{-2}).

This model assumes the mouth pressure to be constant. A more accurate model would consider the oscillating pressure component in the mouth, along with a model of the tunable resonant cavity formed by the vocal tract [Elliott and Bowsher, 1982]. A significant role of the vocal tract has been shown for saxophone playing [Clinch et al., 1982, Guillemain et al., 2010, Fritz, 2005]. But a significant role for trombone, and more generally for brass instruments, has yet to be exhibited [Fréour and Scavone, 2013, Chen et al., 2012].

Nonlinear effects in the resonator should be taken into account to accurately describe the behavior of brass instruments at medium/high playing levels [Hirschberg et al., 1996, Myers et al., 2012] particularly the "brassy sound" related to the formation of shock waves. However, the main objective of this paper is the study of oscillation around threshold (i.e. at low levels), therefore the acoustic propagation along the bore can reasonably be considered linear. Hence, the input impedance is considered enough to describe the resonator.

For this article, input impedances of a Courtois T149 tenor trombone (and when mentioned, a Couesnon "Excelsior" baritone-saxhorn in B^b) have been used. Impedances have been measured with the impedance sensor described in [Macaluso and Dalmont, 2011]. These are fitted by a

sum of complex modes (Lorentzian functions). The characteristic impedance of the resonator is $Z_c = \rho c/S$, with S being the input cross section of the bore at the mouthpiece rim. The modal-fitted impedance is written:

$$Z(\omega) = Z_c \sum_{n=1}^N \frac{C_n}{j\omega - s_n}, \quad (4)$$

s_n and C_n being respectively the poles and the residues of the n^{th} complex mode. Comparison between the measured trombone impedance and an 18-mode fit can be found on fig. 2. The maximum relative difference between fit and measure, for frequencies above 30Hz is lower than 2.6% for the magnitude, and 4.7% for the phase. The measurement in low frequency are slightly biased by the precision of the impedance sensor.

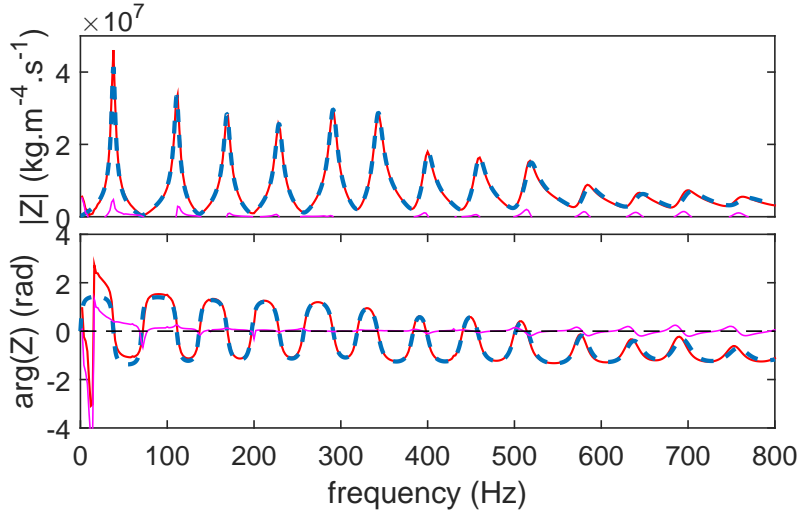


Figure 2: (color online) Magnitude (top) and phase (bottom) of the input impedance of a Courtois tenor trombone. Plain curve depicts the measured impedance, dashed curve is the fitted version with 18 complex modes. The difference between fit and measure is also plotted.

The dynamics of the system described by eq. 2, 3 and 4 can be put in a state-space representation $\dot{X} = F(X)$, where F is a nonlinear vector function, and X the state vector, containing the observables of the system. Taking $p(t) = \sum_{n=1}^N 2\text{Re}(p_n(t))$, where p_n is the n^{th} modal component of the pressure at the input of the bore:

$$\begin{cases} \frac{d^2h(t)}{dt^2} = -\omega_l^2 h(t) - \frac{\omega_l}{Q_l} \frac{dh(t)}{dt} - \frac{p(t)}{\mu} + \omega_l^2 h_0 + \frac{p_b}{\mu} \\ u(t) = \sqrt{\frac{2}{\rho}} L h(t) \sqrt{p_b - p(t)} \\ \frac{dp_n}{dt} = Z_c C_n u(t) + s_n p_n(t) \text{ for } n \in [1 : N]. \end{cases} \quad (5)$$

This leads to the following state vector, similar to the one proposed in [Silva et al., 2014]:

$$X = \left[h(t); \frac{dh}{dt}; p_n(t) \right]_{n \in [1 : N]}. \quad (6)$$

B Choice of lip parameters

Setting the values for the parameters of the lip model is not obvious, as measuring the mechanical impedance (displacement over force ratio) in playing condition seems out of reach. Adjusting parameters to get results comparable with measured signals seems unproductive. Even if a one-DOF model depends on a small number of parameters, different sets of parameters values may lead to similar results. Moreover, contrary to woodwind instrument valves which remain fairly steady regardless of the played note, the lip valve parameters of a trombonist vary while playing. Particularly, the lip resonance frequency is adjusted to select the intended register of the instrument.

A preliminary bibliographical review on lips parameter values has been done. Results from the literature are gathered in table 1 along with a brief "abstract" of the method used in the reviewed articles.

Reference	$h_0(\text{m})$	$L(\text{m})$	$f_l(\text{Hz})$	$1/\mu((\text{m}^2\text{kg}^{-1}))$	Q_l	"Abstract"
[Gilbert and Aumond, 2008]	$5, 8 \cdot 10^{-4}$	$14 \cdot 10^{-3}$	60–260	0.27	0.15–0.037	No information; Variable Q_l value
[Gazengel et al., 2007]						human lip; saxophone-like position; 3 muscular tensions
Soft	N/A	N/A	115.7	N/A	0.79	
Medium	N/A	N/A	479.87	N/A	0.46	
Tight	N/A	N/A	1073	N/A	0.46	
[Cullen et al., 2000]						1 st (Outward) mode artificial lips
Soft	$6, 3 \cdot 10^{-4}$	$18 \cdot 10^{-3}$	189	0,07	10,5	
Medium	$5, 3 \cdot 10^{-4}$	$12 \cdot 10^{-3}$	203,5	0,11	6	
Tight	$4, 4 \cdot 10^{-4}$	$11 \cdot 10^{-3}$	222	0,09	9	
[Newton et al., 2008]	N/A	N/A	32	N/A	1,2–1,8	Human lips High-speed camera
Richards et al. (unpub.)	$5 \cdot 10^{-4}$	$7 \cdot 10^{-3}$	167	0,19	3,7	artificial lips fit for good results
[Elliott and Bowsher, 1982]	N/A	N/A	200	0,2	$0,5 \pm 0,03$	Q_l measured on cheek
[Rodet and Vergez, 1996]	N/A	N/A	428,4	0,67	2,88	Trumpet; adjusted for simulation
[Adachi and Sato, 1996b]	10^{-3}	$7 \cdot 10^{-3}$	60–700	$S(2\pi)^2 f_l / 1.5$	0.5–3	Adj. for simulation

Table 1: Recording of different values of lip parameters from literature, along with a brief explanation of the method. In some articles, certain values are not available (N/A). For papers using 2-DOF lip models, only the first, outward DOF is recorded.

This work completes a similar review performed by M. Newton in his PhD thesis [Newton, 2009, p.119]. Many authors do not give the parameter values they use, nor give explanations about their method to get these values, unless the fact that these parameters allow periodic self-sustained

oscillation of the model. The measures on human or artificial lips were made in conditions as similar as possible to the playing conditions.

Our initial intention was to stick as close as possible to the values measured on natural lips [Gazengel et al., 2007, Newton et al., 2008]. Geometric parameters (width and height at rest of the lip channel) given in all studies are very steady, around $h_0 = 5.10^{-4}\text{m}$ and $L = 12.10^{-3}\text{m}$. Parametric studies performed by the authors have shown that variations of these do not drastically change the qualitative behavior of the model. Similar observations have been made about μ , even if the range of the values gathered is a little wider ($\mu \in [3.7 : 11.1]$ for the trombone).

Measurements from [Gazengel et al., 2007, Newton et al., 2008] tend to give low quality-factor values between 0.5 and 2. However, preliminary analysis carried out with $Q_l \approx 1$ showed very unrealistic pressure thresholds (order of magnitude : 10^4 to 10^5Pa). Thus, an intermediate value for Q_l was chosen, closer to the values measured on artificial lips ($Q_l \in [5 : 10]$).

In all the simulations of this paper, the set of parameters used for simulation and linear stability analysis is given in table 2:

$h_0(\text{m})$	$L(\text{m})$	$1/\mu(\text{m}^2\text{kg}^{-1})$	Q_l
5.10^{-4}	12.10^{-3}	0.11	7

Table 2: Lip parameters retained for the article

C Stability of the equilibrium solution

Linearizing a closed-loop system to assess potential instabilities is a widely used method, as much in the dynamical systems community [Bergé et al., 1995] as in musical acoustics for brasswind, woodwind and flute-like instruments [Wilson and Beavers, 1974, Cullen et al., 2000, Silva et al., 2008, Terrien et al., 2014]. Basically, the equations describing the system are linearized around a known equilibrium solution. Then, the stability of this solution is evaluated.

Considering the system described in section A, the static equilibrium consists in an equilibrium lip opening h_e . This equilibrium position is slightly larger than the lip opening at rest h_0 , due to the constraint of the blowing pressure on the inner face of the lips. Similarly, there is a small static overpressure p_e at the input of the bore of the instrument. Mathematically, this equilibrium is obtained by canceling all time derivatives in the system, as described in appendix A. The value of p_e is obtained by solving:

$$A^3 + \frac{A^2}{\beta} + h_0\mu\omega_l^2 A - \frac{p_b}{\beta} = 0, \quad (7)$$

with $\beta = \frac{LZ(\omega=0)}{\mu\omega_l^2} \sqrt{\frac{2}{\rho}}$. The value of $Z(\omega = 0)$ is taken from the fitted version of the impedance. This equation has 1 or 3 real roots. In the latter case, the smallest real positive root should be considered to compute $p_e = p_b - A^2$ [Silva, 2009], as $Z(\omega = 0)$ is small. The lip channel height at equilibrium h_e is then given by eq. 3 with $\ddot{h} = \dot{h} = 0$.

The linearized function \tilde{F} can be written as:

$$\tilde{F}(X) = F(X_e) + J_F(X_e)(X - X_e), \quad (8)$$

with $J_F(X)$ being the Jacobian matrix of the function F and X_e the state vector at the equilibrium solution. The solutions of $\dot{X} = \tilde{F}(X)$ are under the form :

$$X(t) - X_e = W e^{\lambda t}, \quad (9)$$

where W is a constant vector of same dimension as X .

Thus, the eigenvalues of the Jacobian matrix give information about the stability of the equilibrium solution for a given set of parameters. If at least one of these eigenvalues λ has a positive real part, the amplitude of the linearized solution tends toward infinity, which means the equilibrium is unstable and the solution starts oscillating. In the transient phase of the oscillation, the exponential growth of the amplitude is determined by the positive real part of λ , and the angular frequency is given by the imaginary part of the eigenvalue $\omega = \text{Im}(\lambda)$. However, the nonlinearities of the system limit the final amplitude and also affect the oscillation frequency of the steady state.

This method only allows the detection of instabilities emanating from the equilibrium solution. If a stable oscillating regime coexists along with the stable equilibrium solution, it won't be detected. This situation occurs for example in certain woodwind instruments, where the Hopf bifurcation (connecting the equilibrium solution to the oscillating one) is inverse for certain cases [Farner et al., 2006].

D Time-domain simulation

Another approach for studying musical instruments is solving (numerically) the equations of the chosen model, for a given set of parameters. Results of this resolution are time-domain simulated signals of each observable of the state vector, which also give information on the transient of the signals.

Multiple numerical methods have been developed and used to simulate wind instruments with models similar to the one presented in section A. The primary difference is in the numerical modeling of the acoustics of the resonator. The reflection function of the bore has been widely used [McIntyre et al., 1983, Schumacher, 1981, Adachi and Sato, 1996a, Vergez and Rodet, 1997, Gilbert and Aumond, 2008]. The modal decomposition of the bore has been chosen for this article, and computations are carried out with the open-source MoReeSC software tool, freely available on its website. Principles and results of this library are described in [Silva et al., 2014]. This simulation tool uses a control-theory-like modeling which is similar to the one presented in section A. This eases the numerous comparisons between linear stability analysis results and the behavior of simulated signals. It allows the simulation of the behavior of the model with a high number of acoustic modes for the resonator (18 in this paper), and offers a large flexibility to modify the model parameters, as it will be done in section 4.

III Results

A Linear Stability Analysis

The linear stability analysis method detailed in section C is applied to the model defined in section A, with the set of lip parameters defined in Table 2. The resonator is modeled with a modal fit (N=18 in eq. 4).

For each value of f_l under study (here $f_l \in [20 : 500\text{Hz}]$), the eigenvalues of the Jacobian matrix $J_F(X_e)$ presented in eq. 8 have been computed for increasing values of p_b , until a first instability occurs. Results are reported in Fig. 3. For each value of f_l , the top plot represents the lowest value of p_b giving an unstable equilibrium solution, further referred to as threshold pressure p_{thresh} . The bottom plot represents the imaginary part of the corresponding eigenvalue divided by 2π , which is the oscillation frequency at threshold, further called f_{thresh} . Each horizontal dashed line on this bottom plot represents the n^{th} acoustic resonance frequency of the instrument $f_{ac,n}$ given by the maxima of the input impedance amplitude.

It should be noted that, for p_b values higher than p_{thresh} , other pairs of conjugate eigenvalues may have a positive real part. This means a system with multiple instabilities. If different oscillating solutions are stable with these parameters, the system would be able to start oscillating on different registers. In fig.3 and similar figures, the first instability (the one corresponding to the lowest p_b) is recorded for each f_l value (curve). The second instability is recorded for a smaller range of f_l (dashed curve).

On the [20 : 500Hz] frequency range represented, both plots of Fig. 3 can be divided into 9 ranges of f_l , each corresponding to one regime or register of the instrument: [30 : 63Hz] (first regime), [72 : 123Hz] (second), [124 : 179Hz], [180 : 234Hz], [235 : 288Hz], [289 : 352Hz], [353 : 404Hz], [405 : 460Hz], [462 : > 500Hz]. On the bottom plot, the oscillating frequency f_{thresh} stays on plateaus just above each value of $f_{ac,n}$. This is the usual behavior of an outward valve at threshold, which oscillates at a frequency just above the resonance frequency of the n^{th} acoustic mode of the bore implied in the instability of the equilibrium solution ($f_{thresh} > f_{ac,n}$)[Campbell, 2004]. For each regime, f_{thresh} monotonously follows the variation of f_l . This matches the experience of the brass player, who can slightly "bend" the sound (increase or decrease the pitch) by adjusting f_l through the muscular tension of the lips, and adapting the blowing pressure to the change of p_{thresh} . The width of each plateau, i.e. the attainable musical range on each register, has analytic limits depending on the lip quality factor Q_l as detailed in [Silva et al., 2007].

In terms of p_b , it can be observed in Fig. 3 (top) that the oscillation threshold globally increases with the rank of the register. A greater p_b value is required to reach the higher notes of the instrument, in accordance with the musical experience. Simultaneously to the f_{thresh} plateaus, the oscillation thresholds have U-shaped parts, qualitatively similar with the ones presented in [Silva et al., 2007]. Those U-shapes have a minimum value p_{opt} for each register (indicated by circles) which depends significantly on the losses of the resonator according to [Silva et al., 2007]. In the following, we assume that p_{opt} and the associated lip resonance frequency f_{opt} are the

optimal playing configuration for a human performer. This hypothesis is related to the strategy of musicians, who claim to minimize the effort to produce a sound on a given regime. The p_{opt} values are between $500Pa$ and $10kPa$ of the same order of magnitude as the blowing pressures recorded in our measurements. The pressure threshold increases faster when f_l is above f_{opt} than below (see zoom-box on fig. 3 bottom). These results are compatible with brasswind playing experience, as it requires less effort for a musician to "bend down" a note than "bending" it up.

The following will focus on some examples of $[p_b, f_l]$ points to illustrate the different behaviors observed on the model. For each case, the agreement between the results of the linear stability analysis and the sound produced by the time-domain simulation described in section D will be discussed.

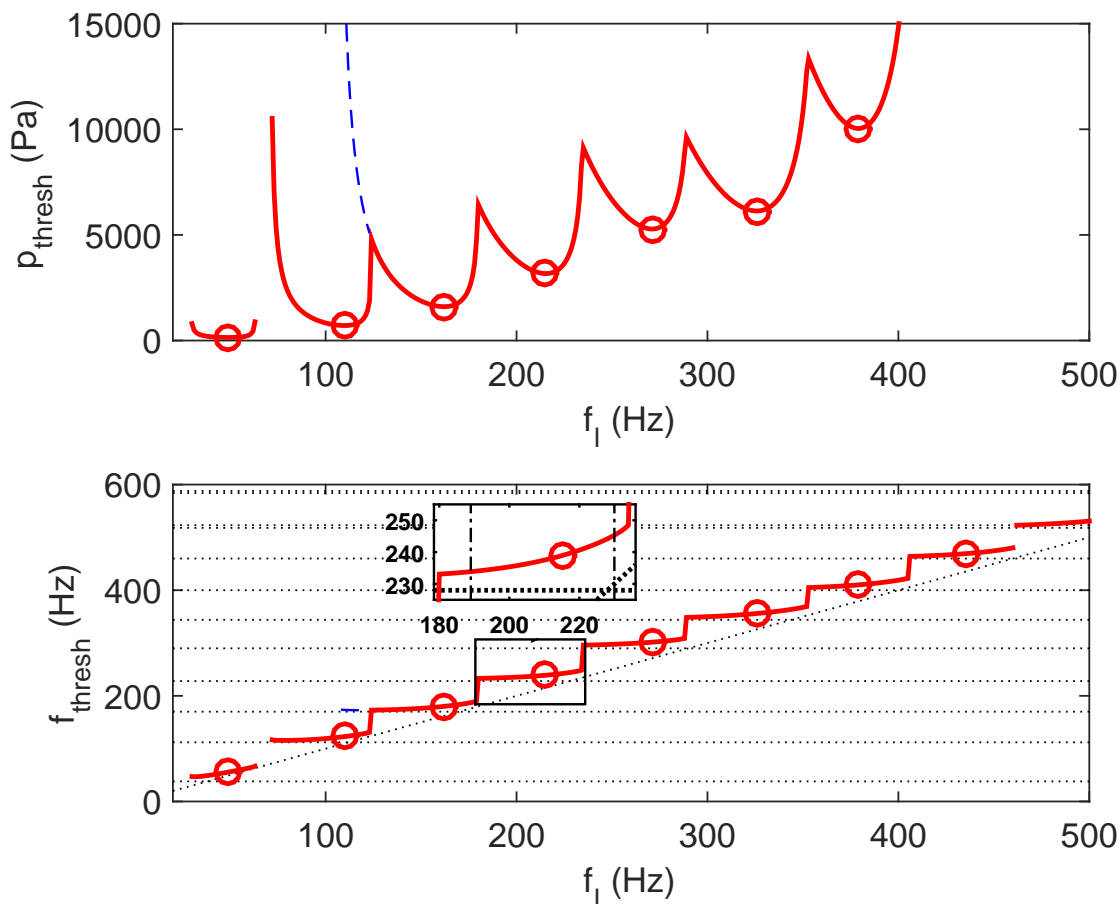


Figure 3: (color online) Results of the linear stability analysis of the model detailed in section A with parameters from table 2. For a range of lip resonance frequency f_l , the top plot presents the threshold mouth pressure p_{thresh} , while the bottom plot shows the corresponding oscillation frequency f_{thresh} . Dotted lines are the values of $f_{ac,n}$. The magnified subplot (zoom on 4th regime) highlights the asymmetrical f_{thresh} behavior above and below p_{opt} . Circles point the "optimal" values p_{opt} and f_{opt} . Thinner dashed lines represent the second destabilization threshold (top) and the corresponding frequency (bottom).

B Exact match between simulation and linear stability analysis

The simulated pressure at the input of the instrument is compared with the LSA results. In particular, the pressure threshold p_{thresh} is assessed by performing simulations with p_b in the vicinity of p_{thresh} . The f_{thresh} values are also compared with f_{osc} . This latter quantity is measured thanks to the instantaneous frequency detection function "Mirpitch" from the MIR toolbox. This MATLAB toolbox contains numerous functions for music information retrieval, including Mirpitch which estimates the frequency of a musical sound.

A simulation with the exact value of p_{thresh} would theoretically lead to infinite transient times (time until the steady state is reached). Therefore, values of p_b slightly below and above p_{thresh} are tested. The chosen lip resonance frequency is $f_l = 90\text{Hz}$, everything else being given in Table 2. The corresponding mouthpiece pressure signals are represented in the two first plots of Fig. 4. The third plot shows a situation where p_b is much higher than p_{thresh} .

When the mouth pressure is a bit below the threshold ($p_b = 1210\text{Pa}$ whereas $p_{thresh} = 1222\text{Pa}$) (Fig 4 left), the oscillation decreases exponentially towards the static, non-oscillating solution. The thick line represents exponential decrease given by eq. 9. In this case, λ is the eigenvalue of J_F with the highest (negative) real part. The calculated oscillation's frequency (dash-dotted line) is constant and equal to $f_{thresh} = 116\text{Hz} = \text{Im}(\lambda)/2\pi$.

When the mouth pressure is slightly above the threshold ($p_b = 1234\text{Pa}$) (Fig 4 center), the signal envelope increases exponentially during the transient phase (also following eq. 9, plotted in thick line) at beginning, before reaching a steady-state regime. The calculated oscillation frequency f_{osc} (dash-dots) begins at $f_{thresh} = 116\text{Hz}$; it becomes quite higher in the permanent regime (126Hz that is 8.6% or 143 musical cents above f_{thresh}).

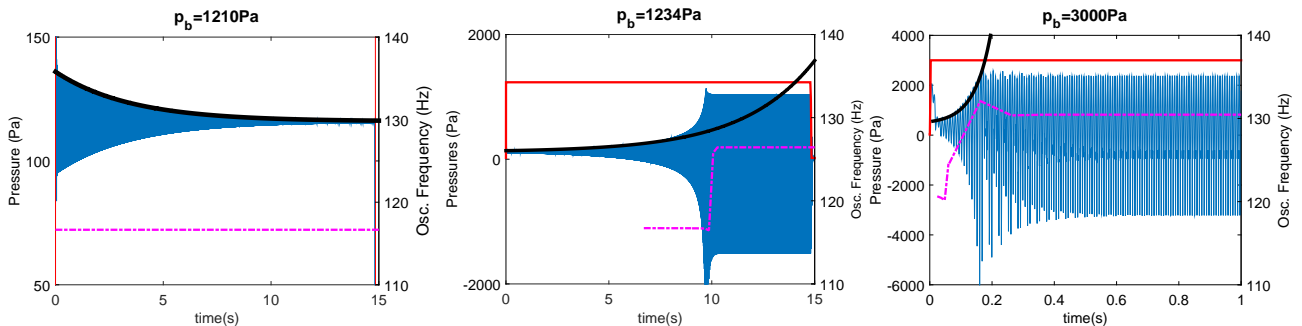


Figure 4: (color online) Time-domain simulations with parameters from table 2 and $f_l = 90\text{Hz}$, with mouth pressure p_b lower (left) and higher (middle) than the linearized model threshold ($p_{thresh} = 1222\text{Pa}$). Mouth pressure (steady) and mouthpiece (oscillating) pressures are plotted (left vertical axis) along with the expected exponential growth/diminution of amplitude (thick curves: envelope of eq. 9). The expected oscillation frequency at threshold is $f_{thresh} = 116\text{Hz}$. The third plot (right) corresponds to a blowing pressure much higher than the threshold ($p_b = 3\text{kPa}$; zoom on first second of signal). The dash-dotted curve depicts the instantaneous playing frequency.

As expected, the behavior of time-domain simulations is accurately predicted by the linear stability analysis as long as p_b remains in the vicinity of the calculated threshold (left and center plot).

p_{thresh} is accurately computed, and the value of the eigenvalue with the largest real part predicts the frequency and the amplitude of the oscillation at the beginning. However, the amplitude gets finally limited by nonlinear phenomena. Thus, this linearized tool is unable to predict the amplitude of the established regime's waveform.

The third plot shows the results with $p_b = 3\text{kPa}$ much higher than p_{thresh} . The two methods still give coherent information, but the oscillating frequency $f_{osc} = 130.5\text{Hz}$ is 8% higher than $Im(\lambda)/(2\pi) = 120.8\text{Hz}$. The difference is 134 musical cents, larger than a semitone. f_{osc} is higher in this situation than near the threshold, which can be correlated with the musical experience: the pitch rises when the player increases its blowing pressure [Campbell and Greated, 1994]. But this remark should be considered cautiously because in practice, the control of mouth pressure and lips muscular activity are always correlated for a brass player.

This example is representative of most cases tested, as the linear stability analysis predicts correctly whether there will be an oscillation or not, with a good estimation of the oscillation frequency at threshold. Moreover, a strong correlation between the duration of the transient and the value of the real part of the unstable eigenvalue has been observed. However this reliability is limited to mouth pressures near the oscillation threshold. On the other hand, the linear stability analysis can predict neither the final amplitude of the permanent regime of oscillation, nor the steady-state waveform. This latest observation will be further highlighted in the following sub-section.

C Unforeseen behaviors

The linear stability analysis provides a lot of pertinent information about the oscillation threshold and the transient phase. This is particularly true when p_b is near p_{thresh} . However, some simulations (detailed below) show nonlinear phenomena, obviously out of reach for this method.

Quasi-periodic oscillations

Firstly, the previous comparison is reproduced with a different lip resonance frequency. Three simulations are performed with the parameters of table 2 and $f_l = 110\text{Hz}$. Now, p_{thresh} is equal to 711Pa. Again, three different p_b values are tested: $p_b = 701\text{Pa}$, $p_b = 720\text{Pa}$ and $p_b = 2\text{kPa}$. Results are plotted on Fig. 5. When p_b is near the threshold, results are very similar to the previous case with $f_l = 90\text{Hz}$ (Fig. 5 left and middle). But when p_b gets large enough, the oscillation of the mouthpiece pressure becomes quasi-periodic (fig. 5 right).

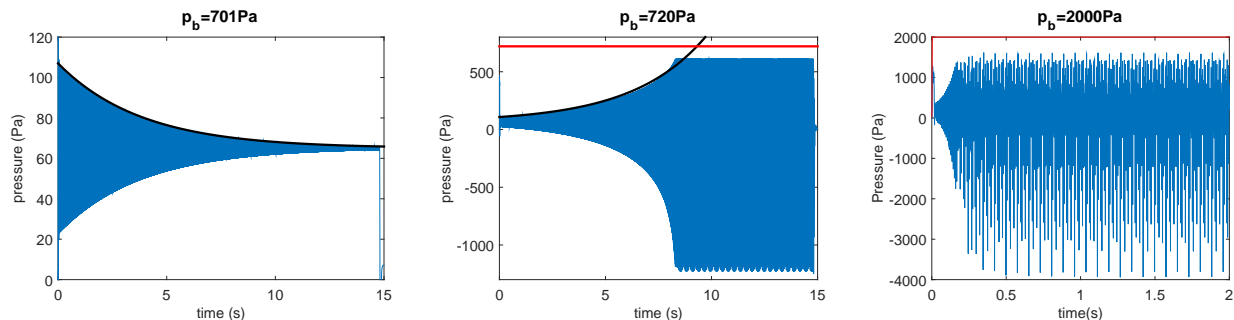


Figure 5: (color online) Simulation results for $f_l = 110\text{Hz}$, the pressure threshold being $p_{thresh} = 711\text{Pa}$. Like in fig. 4 three simulations are shown with $p_b = 701\text{Pa}$ (left), $p_b = 720\text{Pa}$ (middle) and $p_b = 2\text{kPa}$ (right, much higher than p_{thresh}). Other parameters (lip characteristics) are given in Table 2.

This illustrates the aforementioned limitation of linear stability analysis. The existence of an oscillating solution is attested in the vicinity of the bifurcation, and the pressure threshold of the instrument is accurately predicted, but the waveform of the permanent regime is out of reach.

Period doubling

When initialized with $f_l = 55\text{Hz}$, $p_b = 400\text{Pa}$ (p_{thresh} being 161Pa) and the other lip parameters given in Table 2, the time-domain simulation result oscillates at 32.5Hz , significantly under the trombone's first acoustic resonance ($f_{ac,1} = 38\text{Hz}$). This is an unexpected behavior. This oscillation cannot be directly sustained by any acoustic resonance, as the 1-DOF outward valve modeling the lips produces playing frequencies above the acoustic resonance frequency ($f_{osc} > f_{ac,n}$) at least near the pressure threshold, to comply with the regeneration condition [Elliott and Bowsher, 1982].

Figure 6 compares the spectrum of the simulated mouthpiece pressure with the aforementioned parameters (dotted plot) and the f_{thresh} values in a very similar situation, the parameters being the same except $f_l = 50\text{Hz}$, i.e. 5Hz lower (plain plot). When $f_l = 50\text{Hz}$, $f_{osc} = 65\text{Hz}$ is slightly higher than $f_{thresh} = 56.3\text{Hz}$; while for $f_l = 55\text{Hz}$, the simulation's oscillation frequency is very close to the half of f_{thresh} . We conclude that, by increasing progressively f_l , the periodic solution undergoes a flip bifurcation [Bergé et al., 1995]. A quite small variation of the lip resonance frequency can lead to a regime with a sub-harmonic frequency and its harmonics. To the authors knowledge, period doubling had never been observed on a model of brass instruments. However, trombone players whose facial muscles (embouchure) get exhausted by excessive practice sometimes notice their sound being an octave lower than what they expect.

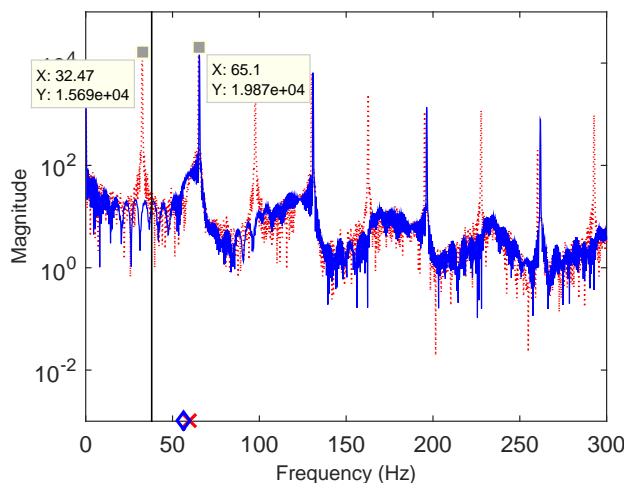


Figure 6: (color online) Spectra of the simulated mouthpiece pressures of a trombone, with ($p_b = 400\text{Pa}$) for both situations, $f_l = 50\text{Hz}$ (plain) and $f_l = 55\text{Hz}$ (dotted) (other parameters from table 2). The values of f_{thresh} are pointed by a diamond ($f_l = 50\text{Hz}$) and a cross ($f_l = 55\text{Hz}$). The plain vertical line indicates the first acoustic resonance frequency of the trombone bore, $f_{ac,1} = 38\text{Hz}$.

Second destabilization

Besides these two nonlinear phenomena, other differences between our linear stability analysis tool and time-domain simulation are possible. A third example is given with $f_l = 120\text{Hz}$, the parameters given in table 2 and a high blowing pressure ($p_b = 6.5\text{kPa}$ while the threshold is $p_{thresh} = 1056\text{Pa}$). While $f_{thresh} = 128.4\text{Hz}$ is just above the 2nd acoustic resonance frequency of the bore ($f_{ac,2} = 112\text{Hz}$), the simulation's oscillation frequency is $f_{osc} = 187.5\text{Hz}$, near the 3rd resonance frequency ($f_{ac,3} = 170\text{Hz}$). Figure 7 shows the spectrum of a simulation oscillating on the third register, while the predicted oscillation at threshold corresponds to the second one.

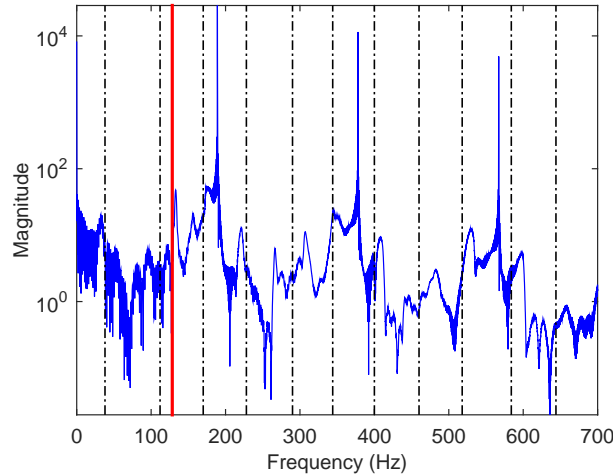


Figure 7: (color online) Spectrum of simulation result for $f_l = 120\text{Hz}$ and $p_b = 6.5\text{kPa}$ with other parameters taken from table 2. The self-sustained oscillation occurs at $f_{osc} = 187.5\text{Hz}$, corresponding to the third register; while linear stability analysis predicts an oscillation at $f_{thresh} = 128.4\text{Hz}$ (plain line) for $p_{thresh} = 1056\text{Pa}$. Each dash-dotted line represents the n^{th} acoustic resonance frequency $f_{ac,n}$ of the trombone bore.

Retaining the lowest p_b which destabilizes the equilibrium solution is not enough, here, to predict the behavior of the system with higher blowing pressure. Yet, this oscillation on the third regime can be detected by recording other pairs of eigenvalues of the Jacobian matrix having a positive real part, for $p_b > p_{thresh}$. The dashed plot on fig 3 shows the pressure threshold corresponding to the second pair of such eigenvalues (noted λ_2), and the associated frequency. For $f_l = 120\text{Hz}$ the second threshold is 6116Pa with an oscillation frequency equal to $Im(\lambda_2)/2\pi = 172\text{Hz}$, corresponding to the simulated third regime. This is consistent with the behavior observed in the numerical simulation.

For a better understanding of the origin of the different instabilities, another approach to perform linear stability analysis may be preferred, as it gives visual information about the stability margins of the different registers. It consists in studying a linearized version of the open-loop transfer function (OLTF) of the system defined by eq. 2, 3 and 4 [Ferrand et al., 2010]. This OLTF is divided into two parts: the exciter's admittance Y_a which describes the lip reed behavior, from eq. 2 and 3, and the resonator, once again modeled with a modal fit of its input impedance Z (see eq. 4).

The linearization of the exciter's admittance Y_a simplifies to a 1st degree Taylor expansion of eq. 2 near the equilibrium point; eq. 3 is then put into the result. Details of the calculation can be found in Appendix B and leads to the following expression of Y_a :

$$Y_a = Lh_e \sqrt{\frac{2p_e}{\rho}} \left(-\frac{D(\omega)}{Kh_e} - \frac{1}{2p_e} \right), \quad (10)$$

where D represent the dynamics of the lip reed (see Appendix B).

The stability of the OLTF, noted H_{OL} , is then studied with the Barkhausen criterion, which points out possibly unstable points when $H_{OL} = Y_a.Z = 1$. On a Bode diagram, unstable points are those of H_{OL} having a 0dB magnitude and 0° phase. This method has already been used for clarinet models with inward valves, and for brass and flute-like instruments [Benade, 1976, Ferrand et al., 2010, Terrien et al., 2014].

Figure 8 shows the Bode diagram of the OLTF of the system fed with the parameters of Figure 7. The unstable points are easily recognized. The computation is fast enough to observe evolution on the Bode plot in real time while modifying a parameter.

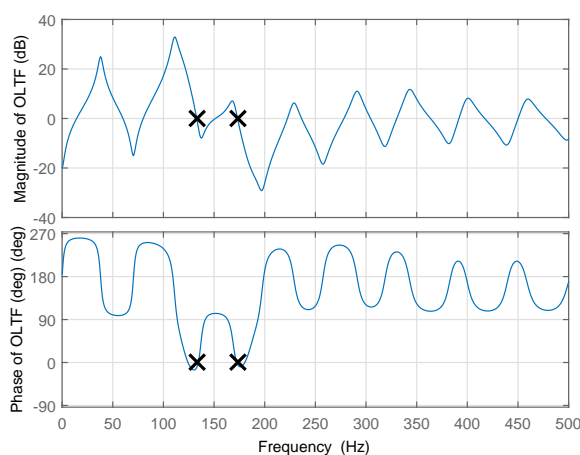


Figure 8: (color online) Bode diagram of the open-loop transfer function of the trombone model with parameters of table 2, $f_l = 120\text{Hz}$ and $p_b = 6.5\text{kPa}$. There are two instability points (crosses), with a 0dB magnitude and a zero phase.

Here, the Bode diagram presents two points of 0dB magnitude and 0° phase, which means two instabilities of the equilibrium solution, at 132Hz and 172Hz. In the terms of the first linear

stability analysis tool described in C, these frequencies correspond to the imaginary part of the eigenvalues of J_F having a positive real part when these are calculated with $p_b = 6500\text{Pa}$. The value obtained with OLTF differs from the one obtained with the first linear stability method, because $f_{thresh} = 128\text{Hz}$ is obtained at $p_b = p_{thresh} = 1056\text{Pa}$ while the OLTF value is obtained with $p_b = 6.5\text{kPa}$. The second destabilization thresholds match well, because the destabilization threshold of the third regime is 6116Pa nearer from $p_b = 6.5\text{kPa}$. This frequency is lower than the actual $f_{osc} = 189\text{Hz}$ value, but it corresponds to the same second regime.

Both linear stability analysis methods show multiple instabilities of the static solution, which means multiple possible regimes of oscillation. But they give neither information about the stability of these regimes, nor about which regime the instrument will actually oscillate on. This is determined by the stability of the different oscillating solutions, which depends on nonlinear elements out of reach of the method.

IV Lowest regime of oscillation

This section focuses on the results of linear stability analysis and time-domain simulation on the lowest register, related to the first acoustic resonance of the air column inside the bore. This lowest playable note is called "pedal note" by musicians. For the trombone with its slide fully pulled in, and the saxhorn with no valve depressed (neutral positions), the pedal note is a B_1^b at 58Hz in the musical scale.

A The Trombone's "pedal note"

To compare more easily the oscillation frequencies of the different registers of the trombone, the ratio between the threshold frequency f_{thresh} and the resonance frequency of the corresponding acoustical mode $f_{ac,n}$ is computed. Fig. 9 gives p_{thresh} and f_{thresh} similarly to fig. 3 on a smaller f_l range, along with the $f_{thresh}/f_{ac,n}$ ratio on the bottom plot.

When focusing on the values at the minimum of pressure threshold f_{opt} (circles) as described in section III, this ratio appears to be significantly higher for the first register than for the other ones: $f_{thresh}/f_{ac,1} = 1.47$ while $f_{thresh}/f_{ac,n} \in [1.04 : 1.09]$ for $n \geq 2$. However, for all the five lowest registers, f_{thresh} is less than 5% from the frequency of the reference note (the note supposed to be played on the instrument for this register, following the tempered scale) when $f_l = f_{opt}$. Given this, the linear stability analysis gives a reliable estimation of the reference note for these registers, including the pedal note.

This high $f_{thresh}/f_{ac,1}$ ratio is coherent with the experience of trombone players, who are able to play a "pedal" B_1^b in tune with the other regimes of oscillation. The trombone's first resonance is at $f_{ac,1} = 38\text{Hz}$ whereas for $n \geq 2$, $f_{ac,n+1} - f_{ac,n} \approx 58\text{Hz}$ which means a major inharmonicity of the lowest resonance compared to the other ones. However, musicians are able to play B_1^b as if there were no inharmonicity [Bouasse, 1986, Velut et al., 2014]. This ability to predict the pedal note of the trombone with the linearization of an outward-valve model is unexpected. It makes

clear that the production of the pedal note involves the same phenomena than the other regimes.

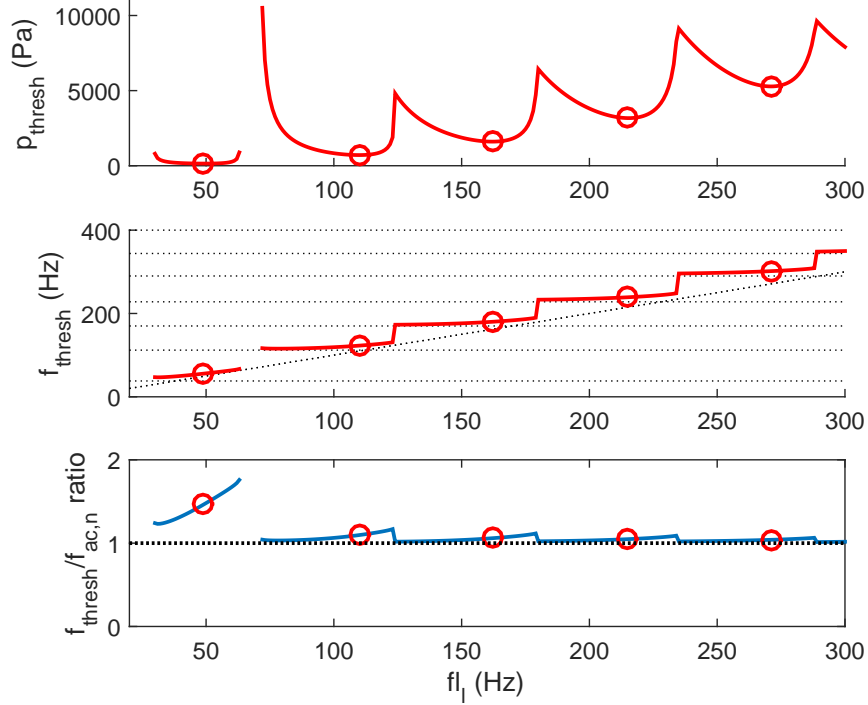


Figure 9: (color online) Results of linear stability analysis (with lip parameters from table 2) are recalled on top and middle plots (narrower f_l range than in fig. 3), along with the $f_{thresh}/f_{ac,n}$ ratio (bottom plot). Circles point the f_{opt} resonance frequencies corresponding to the lowest p_{thresh} .

Bouasse carried out an experiment by playing a trombone with a saxophone mouthpiece [Bouasse, 1986]. Gautier and Gilbert recently reproduced this experiment, with an audio and video recording provided with this paper. The result is an instrument playing a low E_0^b , which means an oscillating frequency just under $f_{ac,1} = 38\text{Hz}$. This experiment is simulated below, and the results presented in fig. 10. The trombone with a saxophone mouthpiece is modeled with a fit of the input impedance of a trombone mounted with the equivalent volume of a saxophone mouthpiece. The saxophone mouthpiece is modeled with an inward-striking valve having the characteristics of a cane-reed, with $f_l = 1\text{kHz}$, $Q = 1.1$; $1/\mu = 4.9\text{m}^2\text{kg}^{-1}$; $L = 10^{-3}\text{m}$; $h_0 = 5.10^{-4}\text{m}$. The oscillating frequency of the simulated mouthpiece pressure sticks to the first resonance frequency ($f_{osc}/f_{ac,1} = 0.99$). The signal is nearly sinusoidal, because of the lack of acoustic resonances matching the harmonics of this frequency.

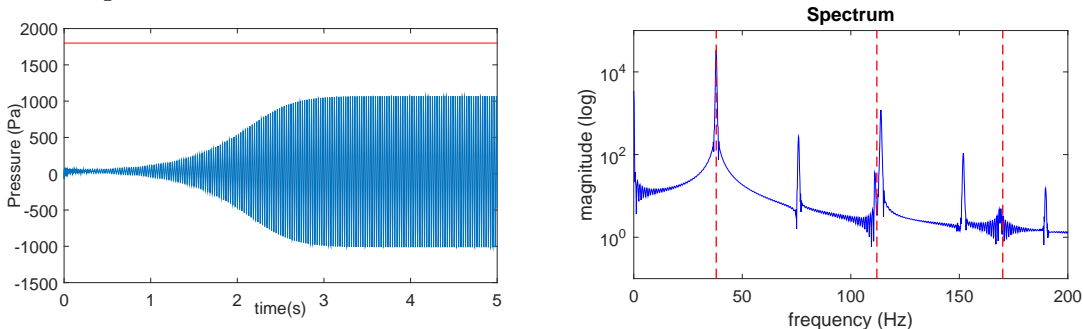


Figure 10: (color online) Results of simulation of a trombone with a tenor saxophone mouthpiece, modeled by an inward-striking valve with reed resonance frequency $f_l = 1\text{kHz}$, $L = 1\text{cm}$, $h_0 = 5.10^{-4}\text{m}$, $Q_l = 1.1$, $1/\mu = 4.9\text{m}^2\text{kg}^{-1}$. The blowing pressure $p_b = 1800\text{Pa}$ is slightly above $p_{thresh} = 1760\text{Pa}$. Left plot shows the blowing pressure (steady) and the mouthpiece pressure (oscillating). Right plot is the spectrum of the mouthpiece pressure, showing an oscillation frequency of $f_{thresh} = 37.85\text{Hz}$ just under the first acoustic resonance $f_{ac,1} = 38\text{Hz}$. Dashed lines represent the resonance frequencies of the bore for comparison.

These results show that the aforementioned high $f_{osc}/f_{ac,1}$ ratio is specific to outward-striking valve. Put together, these results support the 1-DOF outward-striking modeling of a brass player's lips, as it allows to reproduce even unusual behaviors of the instruments like the pedal note.

B A Saxhorn's "ghost note" ?

A complementary exploration was done using the same computation scheme on a Baritone-saxhorn in B^b . This instrument belongs to the family of the tubas, its bore is nearly conical and it is played on the same range as the tenor trombone. Its input impedance is quite similar to that of a trombone, the main difference being on the first resonance peak which is nearly harmonic with the other ones. Thus, contrary to the trombone, the B^b1 pedal note (lowest playable note) is close to the lowest resonance frequency.

The pedal B_1^b is easily playable by a non-beginner musician. However, the authors fortuitously found out another playable note during practice, whose frequency lies between $f_{ac,1}$ and $f_{ac,2}$. Trials have been carried out on different saxhorn models and brands. The note played can be a D_2^b to a E_2^b , which means a frequency ratio $f_{osc}/f_{ac,1}$ between 1.19 and 1.35. We call it the "ghost note" in this paper. Experienced saxhorn players further confirmed the existence, and facility of emission, of this ghost note on many different saxhorns and tubas, including diverse transposing instruments.

Results of the linear stability analysis of the saxhorn model are provided in fig. 11. The model is the same as the one for the trombone, with only a change in the acoustic impedance used (eq. 4). They are similar to those obtained with the trombone, with a particularly high $f_{thresh}/f_{ac,n}$ ratio on the first register. Again focusing on the f_{opt} values (circles on fig. 11), the ratio is $f_{thresh}/f_{ac,1} = 1.23$. Like for the trombone, this ratio is smaller and quite constant for other modes ($f_{thresh}/f_{ac,n} < 1.05$, $n \geq 2$). Time-domain simulation on a saxhorn model on the first register, (with $p_b = p_{opt} + 1\%$, $f_l = f_{opt}$ and other parameters coming from table 2) confirm these values, with $f_{osc}/f_{ac,1} = 1.23$.

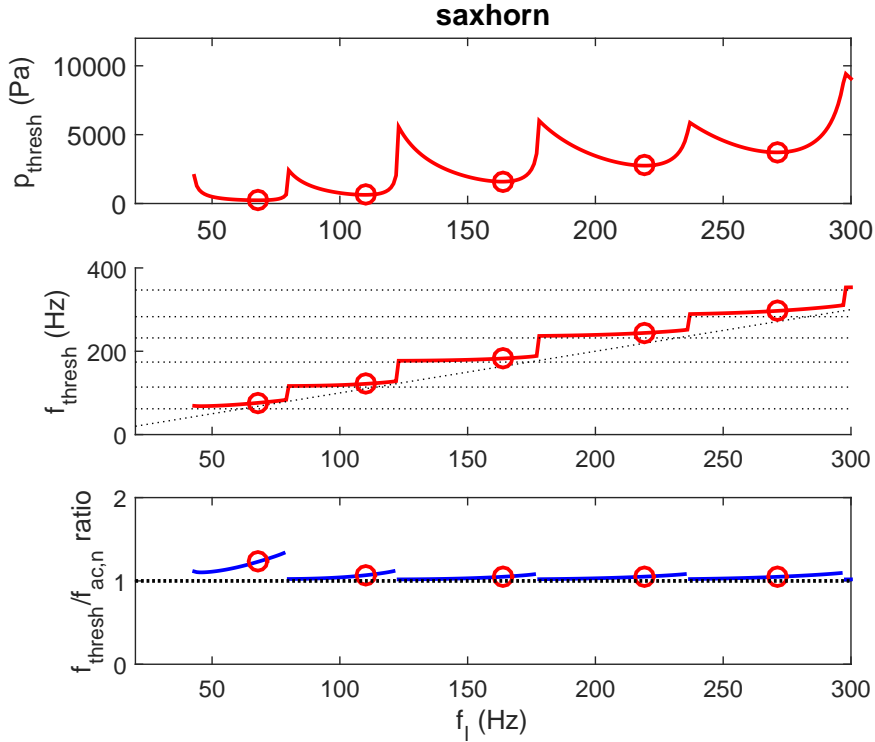


Figure 11: (color online) Results of linear stability analysis (with lip parameters from table 2) of the saxhorn are given under the same form as those of the trombone in fig. 9. Circles point p_{opt} (top) and f_{opt} (bottom).

The gap between the lowest played note and the first acoustic resonance is smaller for the ghost note of the saxhorn ($f_{thresh}/f_{ac,1} = 1.23$) than for the pedal note of the trombone ($f_{thresh}/f_{ac,1} = 1.47$). However, both are significantly higher than for other modes ($f_{thresh}/f_{ac,n} \leq 1.09$ otherwise). Time-domain simulations have been carried out [Velut et al., 2014] with a different set of parameters, that similarly predict a high $f_{osc}/f_{ac,1}$ ratio, higher for the trombone than for the saxhorn. A simple linearized model thus allows to predict the appearance of the pedal note of the trombone and the ghost note of the saxhorn, which is surprising. However, a set of parameters simulating the pedal B_1^b of the saxhorn with this model is yet to be found, if it in fact exists.

C Shift of the lowest resonance of the input impedances

The trombone and the saxhorn give two examples of high $f_{thresh}/f_{ac,1}$ ratios on the lowest register of the instrument. The trombone has a higher ratio than the saxhorn while its first register's resonance frequency is lower. To assess this negative correlation between $f_{ac,1}$ and the $f_{thresh}/f_{ac,1}$ ratio, the first resonance frequency of the input impedance of the considered instruments is changed in the model. This is done by modifying the $\{C_1, s_1\}$ values in eq. 4 while keeping the other modes unchanged, as well as the first mode's amplitude and quality factor.

For each value of $f_{ac,1}$ tested, the $f_{thresh}/f_{ac,1}$ value is recorded at f_{opt} . Results of both saxhorn and trombone are reported on fig. 12. The ratio tends to grow (with a different derivative) when the

resonance frequency tends toward zero. Therefore, the lower $f_{ac,1}$, the larger $f_{thresh}/f_{ac,1}$. Thus, as far as the outward model is concerned, the gap between the playing frequency and the resonance frequency is all the larger as the resonance frequency is low.

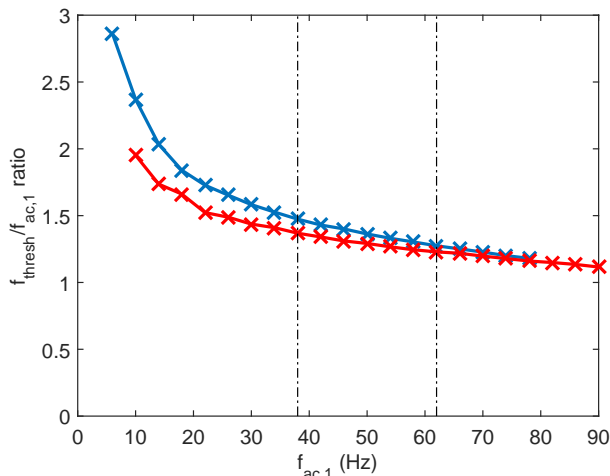


Figure 12: (color online) Ratio between the predicted oscillation frequency f_{thresh} and the acoustic resonance frequency $f_{ac,1}$ for different values of the latter. Plain curve plots the results for the trombone, the dashed one is for saxhorn. All values are taken for $f_l = f_{opt}$. Vertical dash-dotted lines are the original first resonance frequencies of a trombone (38Hz) and a saxhorn (62Hz). For the further registers, $f_{thresh}/f_{ac,n} < 1.09$.

V Conclusions

Most results obtained in this study highlight the usefulness of Linear Stability Analysis (LSA) to understand various near-threshold behaviors of the complete nonlinear model of a brass musical instrument (trombone or saxhorn).

Cases where simulations results are perfectly explained by LSA include obviously exponentially decaying or increasing oscillation transients around the equilibrium solution. Moreover, concerning steady states, periodic regimes are observed at frequencies close to the ones given by LSA, for all registers of the instrument. This remains true as far as the periodic regime emanating from the equilibrium solution remains stable. Indeed, once this periodic regime loses its stability, it gives rise to harmonics switching, quasi-periodicity occurring or period-doubling. Playing other harmonics can be predicted, as multiple instabilities of the equilibrium solution are shown by LSA, but it gives no information on which oscillating solution prevails. This demands further studies of the model with numerical continuation tools, such as AUTO or MANlab [Cochelin and Vergez, 2009]: to detect the bifurcations between oscillation branches and estimate the domain of stability of each periodic solution. Quasi-periodicity and period-doubling are nonlinear phenomena obviously not taken into account in this method.

The most unexpected results of this paper concern the lowest register of brass instruments, but are consistent with musicians' experience. Indeed, in the case of the trombone, linear stability analysis predicts the production of the pedal note. Thus, LSA clearly indicates that for low

enough acoustic resonance frequencies, the frequency of the emerging instability is far beyond the resonance frequency of the instrument. This allows the trombone's pedal note to be played in tune, though the corresponding resonance frequency is misaligned with the nearly harmonic series of the upper peaks of the input impedance. This is an unexpected outcome of LSA, in a way the production of the pedal note involves the same basic phenomena than the other regimes. Considering the saxhorn, LSA also suggests the production of a note - designated as the "ghost note" in this paper - that had never been documented but the playability of which is confirmed by advanced players.

However some questions are still unsolved. First of all, the reason why the ratio between the playing frequency at threshold and the acoustic resonance frequency rises when the latter decreases requires further attention. Moreover, neither LSA nor numerical simulations could explain the production of the pedal note by a saxhorn. This may be due to a limitation of the 1-DOF valve model for the lips or more simply to inadapted parameter values. Indeed, in spite of a bibliographical review carried out in this paper, choosing parameter values for a brass model is challenging. Even if results obtained looks reasonable, consistent with players' experience, in vivo measurements of lip parameters during musical performance would be very valuable.

Acknowledgments

We wish to acknowledge the about ten skilled saxhorn players who confirmed the existence of the ghost note on different instruments. We also wish to thank Fabrice Silva for the discussions about our results and the occasional help for using his MoReeSC software.

This work was done in the framework of Labex MEX (ANR-10-LABX-0092) and of the project A*MIDEX (ANR-11-IDEX-0001-02), funded by the French National Research Agency (ANR).

A Equilibrium point of the system

Prior to apply the linear stability analysis to our model, the equilibrium solution must be computed before linearizing the equations around this solution. This solution consists in a constant lip channel height $h(t) = h_e$, a constant flow between the lips u_e and a constant pressure in the instrument $p(t) = p_e$. Finding these values consists in solving the equation system 5 with these constant values. The system becomes:

$$\begin{cases} 0 = -\omega_l^2 h_e - \frac{p_e}{\mu} + \omega_l^2 h_0 + \frac{p_b}{\mu} \\ u_e = \sqrt{\frac{2}{\rho}} L h_e \sqrt{p_b - p_e} \\ 0 = Z_c C_n u_e + s_n p_{ne} \text{ for } n \in [1 : N]. \end{cases} \quad (11)$$

Considering the relation between $p(t)$ and its components $p_n(t)$, and adding the variable $A = \sqrt{p_b - p_e}$ this becomes:

$$\begin{cases} h_e = h_0 + \frac{A^2}{\mu \omega_l^2} \\ u_e = \sqrt{\frac{2}{\rho}} L h_e A \\ p_e = Z(\omega = 0) u_e. \end{cases} \quad (12)$$

These three equations can now be mixed :

$$\frac{LZ(\omega = 0)}{\mu \omega_l^2} \sqrt{\frac{2}{\rho}} A^3 + A^2 + L h_0 Z(\omega = 0) \sqrt{\frac{2}{\rho}} A - p_b = 0, \quad (13)$$

which leads to eq 7 given in section C.

B Linearization of Open-Loop Transfer Function

This appendix details the calculations leading to the linearized expression of the open-loop transfer function of the model. The linearization of the admittance Y_a simplifies to a 1st degree Taylor expansion of eq. 2 near the equilibrium point:

$$\tilde{u}(p, h) = u(p_e, h_e) + \left[\frac{\partial u}{\partial p}(p_e, h_e) \right] (\delta p(t) - \delta p_e) + \left[\frac{\partial u}{\partial h}(p_e, h_e) \right] (h(t) - h_e).$$

$\delta p = p_b - p(t)$ is the differential pressure through the lips. δp_e and h_e are the equilibrium values of respectively δp and h , i.e. the values giving the equilibrium solution. Like in section C, the h_e value is obtained by computing the roots of a 3rd order polynomial which variable is $X = \sqrt{\delta p}$:

$$X^3 + \frac{X^2}{\beta} + K \cdot h_0 \cdot X - \frac{p_b}{\beta} = 0 \quad \left(\beta = \frac{Z_0 \cdot L}{K} \cdot \sqrt{\frac{2}{\rho}} \right).$$

h_e is given by eq. 3 in static conditions (all time derivative being null):

$$h_e = h_0 + \frac{\delta p_e}{(\mu \cdot \omega_l^2)}.$$

All calculations being done, the linearized expression of the flow between the lips is:

$$\tilde{u}(p, h) = Lh_e \sqrt{\frac{2p_e}{\rho}} \left(\frac{\delta p(t)}{2p_e} + \frac{h(t)}{h_e} - \frac{3}{2} \right). \quad (14)$$

When translated in the frequency domain, the lip movement equation 3 gives the following relation between the oscillating components of the differential pressure $\delta P(\omega)$ and the height of the lip channel $H(\omega)$:

$$H(\omega) = D(\omega) \frac{\delta P(\omega)}{K}, \quad (15)$$

with $D(\omega)$ being the dynamics of the lips:

$$D(\omega) = \frac{1}{1 - \frac{\omega^2}{\omega_l^2} + j \frac{\omega}{\omega_l} q_r}, \quad (16)$$

which leads to this final expression of the valve admittance:

$$Y_a = L \cdot h_e \cdot \sqrt{\frac{2p_e}{\rho}} \left(-\frac{D(\omega)}{K \cdot h_e} - \frac{1}{2 \cdot p_e} \right). \quad (17)$$

C Nomenclature of symbols

The symbols and abbreviations used all along this paper are reminded here, along with their meaning and the unit used:

- $h(t)$: Height of the lip channel (m);
- L : Width of the lip channel (m);
- h_0 : Height of the lip channel at rest (m);
- ρ : Density of air at 20°C ($kg \cdot m^{-3}$);
- μ : Equivalent surfacic mass of the lips ($kg \cdot m^{-2}$);
- Q_l : Quality factor of the lips (no unit);
- $p(t)$ or $P(\omega)$: Pressure at the input of the bore of the instrument (Pa);
- p_b : Blowing pressure (Pa);
- p_{thresh} : Threshold value of p_b , above which the equilibrium solution is unstable (Pa);
- f_{thresh} : Value of f_{osc} at $p_b = p_{thresh}$ (Hz);
- $u(t)$ or $U(\omega)$: Air flow at the input of the instrument ($m^3 \cdot s^{-1}$);

- $Z(\omega)$: Input impedance of the resonator ($kg.m^{-4}.s^{-1}$);
- $\omega_l = 2.\pi.f_l$: resonance frequency of the lips ($Rad.s^{-1}$);
- f_{osc} : Playing frequency of the instrument (Hz);
- $f_{ac,n}$: Acoustic resonance frequency of the n^{th} mode (Hz);
- f_{thresh} : Oscillation frequency at p_{thresh} (Hz).
- p_{opt} : Lowest value of p_{thresh} for a given register (Pa);
- f_{opt} : Value of f_{thresh} at $p_b = p_{opt}$;

References

- Adachi, S. and Sato, M. (1996a). Time-domain simulation of sound production in the brass instrument. *J. Acoust. Soc. Am.*, 97(6):3850–3861.
- Adachi, S. and Sato, M. (1996b). Trumpet sound simulation using a two-dimensional lip vibration model. *J. Acoust. Soc. Am.*, 99(2):1200–1209.
- Benade, A. (1976). *Fundamentals of musical acoustics*. Oxford University Press, 608 pages.
- Bergé, P., Pomeau, Y., and Vidal, C. (1995). *L'ordre dans le chaos: vers une approche déterministe de la turbulence (Order in chaos : towards a deterministic approach of turbulence)*. Hermann, 352 pages.
- Bergeot, B., Almeida, A., Vergez, C., and Gazengel, B. (2013). Prediction of the dynamic oscillation threshold in a clarinet model with a linearly increasing blowing pressure: influence of noise. *Nonlinear Dynamics*, 74(3):591–605.
- Bouasse, H. (1986). *Instruments à vent—tome 1 (wind instruments—Volume 1)*. Librairie Scientifique et Technique Albert Blanchard, Paris, 411 pages.
- Campbell, M. (2004). Brass instruments as we know them today. *Acta Acustica united with Acustica*, 90:600–610.
- Campbell, M. and Greated, C. (1994). *The musician's guide to Acoustics*. Oxford University Press, Oxford, 624 pages.
- Chen, J.-M., Smith, J., and Wolfe, J. (2012). Do trumpet players tune resonances of the vocal tract ? *J. Acoust. Soc. Am.*, 131(1):722–727.
- Clinch, P., Troup, G., and Harris, L. (1982). The importance of the vocal tract resonance in clarinet and saxophone performance. *Acustica*, 50:280–284.

- Cochelin, B. and Vergez, C. (2009). A high-order purely frequency-based harmonic balance formulation for continuation of periodic solutions. *Journal of Sound and Vibration*, 324.
- Cullen, J., Gilbert, J., and Campbell, M. (2000). Brass instruments: Linear stability analysis and experiments with an artificial mouth. *Acta Acustica united with Acustica*, 86:704–724.
- Dalmont, J.-P., Gazengel, B., Gilbert, J., and Kergomard, J. (1995). Some aspects of tuning and clean intonation in reed instruments. *Applied Acoustics*, 46(1):19–60.
- Elliott, S. and Bowsher, J. (1982). Regeneration in brass instruments. *Journal of Sound and Vibration*, 83:181–217.
- Farner, S., Vergez, C., Kergomard, J., and Lizée, A. (2006). Contribution to harmonic balance calculations of self-sustained periodic oscillations with focus on single-reed instruments. *J. Acoust. Soc. Am.*, 119(3):1794–1804.
- Ferrand, D., Vergez, C., and Silva, F. (2010). Seuils d’oscillation de la clarinette: validité de la représentation excitateur-résonateur (oscillation thresholds of the clarinet: validity of the exciter-resonator representation). In *Proceedings of 10^{eme} Congrès Français d’Acoustique*.
- Fletcher, N. (1993). Autonomous vibration of simple pressure-controlled valves in gas flows. *J. Acoust. Soc. Am.*, 93(4):2172–2180.
- Fréour, V. and Scavone, G. (2013). Acoustical interaction between vibrating lips, downstream air column, and upstream airways in trombone performance. *J. Acoust. Soc. Am.*, 134(5):3887–3898.
- Fritz, C. (2005). *La clarinette et le clarinettiste: influence du conduit vocal sur la production du son (The clarinet and the player: role of the vocal tract on the sound production)*. PhD thesis, Université Paris 6 and New South Wales, France.
- Gazengel, B., Guimezanes, T., Dalmont, J.-P., Doc, J., Fagart, S., and Léveillé, Y. (2007). Experimental investigation of the influence of the mechanical characteristics of the lip on the vibrations of the single reed. In *Proceedings of ISMA 2007*, Barcelona.
- Gilbert, J. and Aumond, P. (2008). Pedal notes of brass instruments, a mysterious regime of oscillation. In *Proceedings of Acoustics’ 08*, Paris.
- Gilbert, J., Kergomard, J., and Ngoya, E. (1989). Calculation of the steady-state oscillations of a clarinet using the harmonic balance technique. *J. Acous. Soc. am.*, 86(1):35–41.
- Guillemain, P., Vergez, C., Ferrand, D., and Farcy, A. (2010). An instrumented saxophone mouthpiece and its use to understand how an experienced musician plays. *Acta Acustica United with Acustica*, 96:622–634.
- Hirschberg, A., Gilbert, J., Msallam, R., and Wijnands, P. (1996). Shock waves in trombones. *J. Acoust. Soc. Am.*, 99:1754.

- Hirschberg, A., Kergomard, J., and Weinreich, G. (1995). *Mechanics of musical instruments*. Springer-Verlag, Wien, Austria.
- Karkar, S., Vergez, C., and Cochelin, B. (2012). Oscillation threshold of a clarinet model: a numerical continuation approach. *J. Acoust. Soc. Am.*, 131(1):698–707.
- Macaluso, C. and Dalmont, J.-P. (2011). Trumpet with near-perfect harmonicity: Design and acoustic results. *J. Acoust. Soc. Am.*, 129(1):404–414.
- McIntyre, M., Schumacher, R., and Woodhouse, J. (1983). On the oscillations of musical instruments. *J. Acoust. Soc. Am.*, 74(5):1325–1345.
- Menguy, L. and Gilbert, J. (2000). Weakly non-linear gas oscillations in air-filled tubes: solutions and experiments. *Acta Acustica United with Acustica*, 86:789–810.
- Myers, A., Pyle, R., Gilbert, J., Campbell, M., Chick, J., and Logie, S. (2012). Effects of nonlinear sound propagation on the characteristic timbres of brass instruments. *J. Acoust. Soc. Am.*, 131(1):678–688.
- Newton, M. (2009). *Experimental Mechanical and Fluid Mechanical Investigations of the Brass Instrument Lip-reed and the Human Vocal Folds*. PhD thesis, University of Edinburgh.
- Newton, M., Campbell, M., and Gilbert, J. (2008). Mechanical response measurements of real and artificial brass players lips. *J. Acoust. Soc. Am.*, 123(1):EL14–EL20.
- Rodet, X. and Vergez, C. (1996). Physical models of trumpet-like instruments. detailed behavior and model improvements. In *Proceedings of ICMC*, pages 448–453, Hong-Kong.
- Schumacher, R. (1981). Ab initio calculations of the oscillations of a clarinet. *Acta Acustica united with Acustica*, 48(2):71–85.
- Silva, F. (2009). *Émergence des auto-oscillations dans un instrument de musique à anche simple (Emergence of self-sustained oscillations in a single reed music instrument)*. PhD thesis, Université de Provence Aix-Marseille 1.
- Silva, F., Kergomard, J., and Vergez, C. (2007). Oscillation thresholds for "striking outwards" reeds coupled to a resonator. In *Proceedings of ISMA 2007*, Barcelona.
- Silva, F., Kergomard, J., Vergez, C., and Gilbert, J. (2008). Interaction of reed and acoustic resonator in clarinet-like systems. *J. Acoust. Soc. Am.*, 124(5):3284–3295.
- Silva, F., Vergez, C., Guillemain, P., Kergomard, J., and Debut, V. (2014). MoReeSC : a framework for the simulation and analysis of sound production in reed and brass instruments. *Acta Acustica United with Acustica*, 100(1):126–138.

- Taillard, P., Kergomard, J., and Laloë, F. (2010). Iterated maps for clarinet-like systems. *Non-linear Dynamics*, 62:253–271.
- Terrien, S., Vergez, C., and Fabre, B. (2014). To what extent can a linear analysis predict the behaviour of a flute model? In *Proceedings of International Symposium on Musical Acoustics*, Le Mans, France.
- Velut, L., Vergez, C., Gilbert, J., and Silva, F. (2014). Numerical simulation of the production of pedal notes in brass instruments. In *Proceedings of International Symposium on Musical Acoustics*, Le Mans, France.
- Vergez, C. and Rodet, X. (1997). Model of the trumpet functioning: Real-time simulation and experiments with an artificial mouth model. In *Proc. of International Symposium on Musical Acoustics (ISMA) 1997*, Edimburgh, Scotland.
- von Helmholtz, H. (1954). *On the Sensations of Tone*. Dover Publications Inc., New York, 608 pages.
- Wilson, T. and Beavers, G. (1974). Operating modes of the clarinet. *J. Acoust. Soc. Am.*, 56(2):653–658.
- Yoshikawa, S. (1995). Acoustical behavior of brass player’s lips. *J. Acoust. Soc. Am.*, 97(3):1929–1939.